IAI Journals.ASM.org

Role of Mouse Peptidoglycan Recognition Protein PGLYRP2 in the Innate Immune Response to *Salmonella enterica* Serovar Typhimurium Infection *In Vivo*

Jooeun Lee,[a] Kaoru Geddes,[b] Catherine Streutker,[c] Dana J. Philpott,[b] and Stephen E. Girardin[a]

Department of Laboratory Medicine and Pathobiology[a] and Department of Immunology,[b] University of Toronto, Toronto, Ontario, Canada, and St. Michael's Hospital, Toronto, Ontario, Canada[c]

Peptidoglycan recognition proteins (PGRPs) are a family of innate pattern recognition molecules that bind bacterial peptidoglycan. While the role of PGRPs in *Drosophila* innate immunity has been extensively studied, how the four mammalian PGRP proteins (PGLYRP1 to PGLYRP4) contribute to host defense against bacterial pathogens *in vivo* remains poorly understood. PGLYRP1, PGLYRP3, and PGLYRP4 are directly bactericidal *in vitro*, whereas PGLYRP2 is an *N*-acetylmuramyl-L-alanine amidase that cleaves peptidoglycan between the sugar backbone and the peptide stem. Because PGLYRP2 cleaves muramyl peptides detected by host peptidoglycan sensors Nod1 and Nod2, we speculated that PGLYRP2 may act as a modifier of Nod1/Nod2-dependent innate immune responses. We investigated the role of PGLYRP2 in *Salmonella enterica* serovar Typhimurium-induced colitis, which is regulated by Nod1/Nod2 through the induction of an early Th17 response. PGLYRP2 did not contribute to expression of Th17-associated cytokines, interleukin-22 (IL-22)-dependent antimicrobial proteins, or inflammatory cytokines. However, we found that *Pglyrp2*-deficient mice displayed significantly enhanced inflammation in the cecum at 72 h postinfection, reflected by increased polymorphonuclear leukocyte (PMN) infiltration and goblet cell depletion. *Pglyrp2* expression was also induced in the cecum of *Salmonella*-infected mice, and expression of green fluorescent protein under control of the *Pglyrp2* promoter was increased in discrete populations of intraepithelial lymphocytes. Lastly, $Nod2^{-/-}$ $Pglyrp2^{-/-}$ mice displayed increased susceptibility to infection at 24 h postinfection compared to $Pglyrp2^{-/-}$ mice, which correlated with increased PMN infiltration and submucosal edema. Thus, PGLYRP2 plays a protective role *in vivo* in the control of *S.* Typhimurium infection through a Nod1/Nod2-independent mechanism.

Innate immunity, the first line of defense against microorganisms, relies on pattern recognition molecules (PRMs), such as Toll-like receptors (TLRs) or nucleotide-binding and oligomerization domain (Nod)-like receptors (NLRs), which initiate protective responses against pathogens by detecting microbe-associated molecular patterns (MAMPs) (6). In the intestine, mucosal defense against enteric pathogens critically depends on the expression of TLRs and NLRs (35), and these PRMs also contribute to the establishment of a homeostatic control of the intestinal microbiota (23, 27).

Peptidoglycan is an essential component of the cell wall of virtually all bacteria and is sensed by a variety of PRMs in the mammalian host, including Nod1, Nod2, and peptidoglycan recognition proteins (PGRPs) (13, 28). Nod1 and Nod2 are two well-characterized members of the NLR family that detect peptidoglycan-derived muramyl peptides (7). Specifically, Nod1 detects *meso*-DAP (diaminopimelic acid)-containing muramyl tripeptides found mostly in Gram-negative bacteria (3, 11), whereas Nod2 recognizes muramyl dipeptide (MDP), a peptidoglycan motif found in both Gram-negative and Gram-positive bacteria (12, 16). PGRPs, first identified in silkworm (41), are conserved from insects to mammals and are characterized by their ability to bind peptidoglycan (28). In mammals, there are four PGRPs, namely, PGLYRP1, PGLYRP2, PGLYRP3, and PGLYRP4 (PGLYRP1-4; initially named PGRP-S, -L, -Iα, and -Iβ, respectively). PGRPs are all capable of binding peptidoglycan (28); PGLYRP1, PGLYRP3, and PGLYRP4 are directly bactericidal (18, 20, 33, 38) but have no amidase activity (18, 20, 39), whereas PGLYRP2 is an *N*-acetylmuramyl-L-alanine amidase that hydrolyzes peptidoglycan between the sugar backbone and the peptide chain (10, 39).

PGLYRP2 is constitutively expressed in the liver, where it is secreted into the blood (40, 43), and its expression is induced by bacteria and cytokines in the skin and in epithelial cells, including those that line the intestinal tract (34, 37). Interestingly, based on the fact that PGLYRP2 cleaves muramyl peptides that are also detected by Nod1 and Nod2, it is possible that this PGRP protein could act as a modulator of Nod-dependent responses. In *Drosophila*, PGRP-LB also has amidase activity, which was shown to protect the host from excessive immune responses by reducing the biological activity of peptidoglycan (25, 42). However, it remains unclear whether the amidase activity of mammalian PGLYRP2 plays a similar anti-inflammatory scavenger function *in vivo* in response to bacterial pathogens.

Despite the fact that PGRPs specifically bind bacterial peptidoglycan and that some of them display antibacterial activity *in vitro* (20, 32, 33, 38), the *in vivo* role of these molecules in host defense against bacterial pathogens remains poorly understood in mammals. One study showed a requirement for PGLYRP1 in re-

Received 15 February 2012 Returned for modification 8 March 2012
Accepted 10 May 2012
Published ahead of print 21 May 2012
Editor: A. J. Bäumler
Address correspondence to Stephen E. Girardin, Stephen.girardin@utoronto.ca.

doi:10.1128/IAI.00168-12

sistance to some infections in mice as *Pglyrp1*-deficient mice showed increased susceptibility to systemic infection with *Bacillus subtilis* and *Micrococcus luteus* but not with other Gram-positive bacteria (*Staphylococcus aureus*) and Gram-negative bacteria (*Escherichia coli*) (5). More recently, another study suggested a role of PGLYRP1 in host resistance against *Listeria monocytogenes* through the induction of tumor necrosis factor (TNF) (24). Similarly, using recombinant PGLYRP3 in wild-type mice, a bactericidal role of PGLYRP3 in preventing *S. aureus* lung infection in mice has also been suggested (20). In contrast, PGLYRP2 was suggested to be redundant for immunity in mice on the basis of the fact that *Pglyrp2*-deficient mice had a normal response to intraperitoneal infection with Gram-positive (*S. aureus*) or Gram-negative (*E. coli*) bacteria (40). It is possible that the four mammalian PGRP proteins display some redundant functions in innate immunity, thus resulting in mild phenotypes for mice lacking any of these molecules. In support for this, in a dextran sulfate sodium (DSS)-induced colitis model, all four individual PGRP knockout mice displayed relatively similar increased sensitivities to DSS and altered immune responses (29). However, PGLYRP2 is unique among mammalian PGRP proteins in that it is the only mammalian protein known to have *N*-acetylmuramyl-L-alanine amidase activity against peptidoglycan, and this protein is one of the most abundantly secreted enzymes in the body fluids of mammals (36). We therefore speculated that PGLYRP2 might have a unique role in host defense that had not been identified previously using *in vitro* assays or intraperitoneal infection models, such as a role in mucosal innate immune defense.

Salmonella enterica serovar Typhimurium (SL1344) causes acute colitis in humans while the same organism causes a systemic disease with little or no intestinal inflammation in mice (15). However, when mice are pretreated with the antibiotic streptomycin prior to infection with *S.* Typhimurium, they develop an acute inflammatory response in the cecum (15). Recently, Nod1 and Nod2 have been shown to modulate inflammation in the streptomycin-treated mouse model of *Salmonella* colitis (8). Given that PGLYRP2 recognizes and hydrolyzes peptidoglycan fragments that are also detected by Nod1 and Nod2 and because mammalian PGLYRP2 is expressed in the intestine (4, 29), we hypothesized that PGLYRP2 may play an important role in modulating Nod1 and Nod2 (Nod1/2)-dependent inflammation in the gut. Therefore, we investigated the role of PGLYRP2 in a murine model of *S. enterica* serovar Typhimurium colitis.

MATERIALS AND METHODS

Mice. *Pglyrp2*-deficient (*Pglyrp2*$^{-/-}$ [KO]) mice were originally obtained from Richard Locksley, and C57BL/6 (wild-type [WT]) mice were purchased from Charles River Laboratories (Wilmington, MA). All mice were bred and housed under specific-pathogen-free conditions in the animal facility of the Center for Cellular and Biomolecular Research, Toronto, Canada. All animal experiments were approved by the Animal Ethics Review Committee of the University of Toronto. In order to minimize variables affecting the outcome of this study, C57BL/6 WT mice were first crossed with fully backcrossed *Pglyrp2*$^{-/-}$ mice (40) to generate heterozygous F1 littermates, and subsequently these F1 mice were crossed again to generate F2 littermates. Genotyping F2 littermates was performed using the following primer sets: for the WT, 5′-GGCTCTCTACTCCCACACAACC-3′ and 5′-GCAGCAATCCAAGCACGATCC-3′; for *Pglyrp2*, 5′-GGCTCTCTACTCCCACACAACC-3′ and 5′-GCCGGACACGCTGAACTTGTGG-3′. WT and *Pglyrp2*$^{-/-}$ mice generated from littermates were used in all our infection studies, and *Pglyrp2*$^{+/-}$ mice were used to study green fluorescent protein-PGLYRP2 expression by flow cytometry.

Nod1$^{-/-}$ *Pglyrp2*$^{-/-}$ double knockout (DKO) and *Nod2*$^{-/-}$ *Pglyrp2*$^{-/-}$ DKO mice were generated by crossing either *Nod1*$^{-/-}$ (Millennium Pharmaceuticals) or *Nod2*$^{-/-}$ mice (Jean-Pierre Hugot [1]) with *Pglyrp2*$^{-/-}$ mouse littermates generated from above. Genotyping was carried out using the following primer sets: for *Nod1*, 5′-CTTAGGCATGACTCCCTCCTGTCG-3′, 5′-GATCTTCAGCAGTTTAATGTGGGAGTGAC-3′, and 5′-CCATTCAGGCTGCGCAACTGTTG-3′; for *Nod2*, 5′-AACCGCATTATTCGATGGGGC-3′, 5′-GTCATTTCCTGACCTCTGACC-3′, and 5′-GCCTGCTCTTTACTGAAGGCTC-3′.

Bacterial infections. WT and *Pglyrp2*$^{-/-}$ mice, 8 to 10 weeks old, were fasted for 3 h prior to oral administration of 20 mg of streptomycin. Mice were again fasted for 3 h after 21 h following streptomycin treatment, and then infected via oral gavage with 5×10^7 CFU of SL1344, a streptomycin-resistant strain of *S. enterica* serovar Typhimurium. Overnight cultures of SL1344 were washed with phosphate-buffered saline (PBS), diluted to the desired CFU level based on optical density readings at 600 nm, and used for infections.

Pathological scoring. The distal halves of cecum samples were collected for histology after mice were sacrificed, fixed in 10% formalin, and then stained with hematoxylin and eosin (H&E) at the Toronto Center of Phenogenomics by standard histological staining procedures. H&E-stained cecum samples were then analyzed in a blinded manner by a pathologist specializing in intestinal inflammation. The scoring system was based on a previous publication (2) that was slightly modified to make the scoring of neutrophil (polymorphonuclear leukocyte [PMN]) recruitment and goblet cell depletion more empirical (8).

Bacterial load quantification. The spleen and cecal tissue samples were collected from infected mice and placed in PBS containing 1% Triton X-100 and in PBS alone, respectively, and then homogenized using a rotor homogenizer. A small (10-μl) cecal sample was further diluted in PBS containing 1% Triton X-100. Both splenic and cecal samples were then serially diluted in PBS and plated on MacConkey agar containing 50 μg/ml streptomycin.

Quantitative real-time PCR. Cecum samples for quantitative reverse transcription-PCR (qRT-PCR) were collected and stored in RNAlater (Sigma), and then RNA was extracted with Qiagen RNeasy extraction kits. Genomic DNA was digested with Turbo DNase (Ambion) before reverse transcription to cDNA with SuperScript RTIII (Invitrogen). qRT-PCR was performed with SYBR green (Applied Biosystems). The following primer sequences, which have been described elsewhere, were used in the current study: *Il17a*, 5′-GCTCCAGAAGGCCCTC-3′ (forward); AGA-3′, 5′-CTTTCCCTCCGCATTGACA-3′ (reverse); *Il22*, 5′-TCCGAGGAGTCAGTGCTAAA-3′ (forward) and 5′-AGAACGTCTTCCAGGGTGAA-3′ (reverse); housekeeping gene *Rpl19*, 5′-GCATCCTCATGGAGCACAT-3′ (forward) and 5′-CTGGTCAGCCAGGAGCTT-3′ (reverse); *RegIII*γ, 5′-ATGGCTCCTATTGCTATGCC-3′ (forward) and 5′-GATGTCCTGAGGGCCTCTT-3′ (reverse); *Lcn2*, 5′-ACATTTGTTCCAAGCTCCAGGGC-3′ (forward) and 5′-CATGGCGAACTGGTTGTAGTCCG-3′ (reverse); *Il1*β, 5′-TTGACGGACCCCAAAAGATG-3′ (forward) and 5′-AGAAGGTGCTCATGTCCTCAT-3′ (reverse); *KC*, 5′-ACTGCACCCAAACCGAAGTC-3′ (forward) and 5′-CAAGGGAGCTTCAGGGTCAA-3′ (reverse); *Pglyrp2*, 5′-ACCAGGATGTGCGCAAGTGGGAT-3′ (forward) and 5′-AGTGACCCAGTGTAGTTGCCCA-3′ (reverse). Values were calculated using the ΔC_T (where C_T is threshold cycle)method and were normalized to the housekeeping gene *Rpl19*.

IEL and LPL isolation. Cecal intestinal intraepithelial leukocytes (IELs) and lamina propria lymphocytes (LPLs) were prepared using a previously established protocol (9). Briefly, cecal tissues were extracted, washed, and cut into 1- to 2-cm segments which were incubated three times (at 37°C for 10 min with shaking) in stripping buffer (PBS, 1% fetal bovine serum [FBS], 5 mM EDTA, 1 mM dithiothreitol [DTT]). After each incubation, the buffer was filtered through a 100-μm cell strainer and then allowed to settle. Supernatants (IELs) were then collected,

washed twice in Dulbecco's modified Eagle's medium ([DMEM] supplemented with 20% FBS) and passed through a 40-μm cell strainer. For LPL extraction, the tissue segments following stripping were minced and put in digestion buffer (DMEM, 20% FBS, 2 mg/ml collagenase D [Roche], 20 μg/ml DNase I [Sigma]) for two 30-min incubations with shaking at 37°C. Digested material was passed through a 100-μm cell strainer, and the cells were collected by centrifugation (5 min at 1,200 rpm), washed twice in DMEM, and then passed through a 40-μm cell strainer to obtain LPLs.

Flow cytometry. Dead cells were stained with Live/Dead Aqua (Invitrogen), and then LPLs and IELs were stained for the surface antigens CD8, CD4, T-cell receptor β (TCRβ), TCRγδ, CD11c, CD11b, major histocompatibility complex class II (MHC-II), CD19, NK1.1, and Gr1 and analyzed for GFP expression. All flow cytometric analyses were performed using an LSR II (BD Bioscience) flow cytometer and analyzed with FlowJo software (TreeStar).

Statistical analyses. The results are given as means ± standard error of mean. Student's *t* tests were performed using GraphPad Prism, and *P* values of <0.05 using a 95% confidence interval were considered significant.

RESULTS

PGLYRP2 is constitutively expressed in some subsets of IELs and LPLs in the cecum. *Pglyrp2* mRNA expression in the total intestinal tissues has been previously described (29). In addition, *Pglyrp2* expression was recently characterized in small intestinal intraepithelial leukocytes (IELs), with the majority of its expression in T lymphocytes (4). Here, we focused on the cecum since this portion of the intestine was recently found to be critical for Nod1/2-dependent control of enteric bacterial pathogens (8, 9). The *Pglyrp2*-deficient (*Pglyrp2*$^{-/-}$) mice used in this study express green fluorescent protein (GFP) under the control of the *Pglyrp2* promoter (40), and therefore we used flow cytometry to monitor PGLYRP2 expression in cecal IELs and lamina propria lymphocytes (LPLs) by tracking GFP expression in *Pglyrp2*$^{+/-}$ mice (to avoid a possible effect on immune cell populations that may occur due to loss of PGLYRP2 expression in *Pglyrp2*$^{-/-}$ mice). At steady state, we confirmed the previously reported high expression levels of PGLYRP2 in lymphocytes from liver and spleen (data not shown) (4). We also detected strong expression of GFP-positive (GFP$^+$) cells in the IELs of the cecum, mainly in CD4$^+$ TCRβ$^+$ (49.7%) and CD8$^+$ TCRβ$^+$ (73.5%) lymphocytes and natural killer cell (NK1.1$^+$ TCRβ$^-$; 76.2%) and natural killer T cell (NK1.1$^+$ TCRβ$^+$; 71.4%) populations (Fig. 1A and Table 1). In contrast to a previous report where PGLYRP2 expression was found to be restricted to T lymphocytes from intestinal IELs (4), we observed that dendritic cells (CD11c$^+$ MHC-II$^+$; 49.7%) and inflammatory monocytes (CD11b$^+$ CD11c$^+$; 23.5%) from the cecal IEL compartment also exhibited various degrees of GFP expression (Fig. 1A and Table 1). Conversely, minimal GFP expression was observed in a CD19$^+$ (3.9%) subset from IELs, indicating the absence of reporter gene expression by B lymphocytes. Moreover, no significant GFP expression was noted in CD11b$^+$ CD11c$^-$ (granulocytes/macrophage/neutrophil) cells (data not shown), and further staining with a Gr1 marker indicated that neither neutrophils (CD11b$^+$ CD11c$^-$ Gr1$^+$; 1.7%) nor macrophages (CD11b$^+$ CD11c$^-$ Gr1$^-$; $<1.0\%$) expressed significant levels of GFP at baseline (Table 1). Similar results were obtained for cecal LPLs, except in NK1.1$^+$ TCRβ$^+$ (1.95%), CD11c$^+$ MHC-II$^+$ ($<1.0\%$), and CD11b$^+$ CD11c$^+$ ($<1.0\%$) cells, where no significant GFP expression was detected (Fig. 1B and Table 1). Overall, PGLYRP2 is constitutively expressed by various leukocytes from the cecum.

PGLYRP2 expression is increased in the cecum during late inflammatory responses against SL1344 infection. PGLYRP2 expression is induced in intestinal epithelial cells and fibroblasts by bacteria and cytokines (21, 34, 37). Thus, we aimed to analyze whether PGLYRP2 expression changed following oral infection with *S. enterica* serovar Typhimurium SL1344. To this end, C57BL/6 wild-type (WT) (KO) mice were treated with streptomycin and infected with 5×10^7 CFU of the streptomycin-resistant *Salmonella* strain, SL1344. We performed quantitative real-time PCR (qRT-PCR) on the cecum samples from the WT mice following SL1344 infection to determine *Pglyrp2* mRNA expression. Although no difference in expression was observed at 24 h, the level of *Pglyrp2* showed approximately 1.7- and 2.3-fold increases at 48 h ($P = 0.02$) and 72 h ($P = 0.03$) postinfection (p.i.), respectively, compared to the uninfected controls (Fig. 2A). In order to determine which cell types contributed to the increase in *Pglyrp2* expression, we analyzed IELs and LPLs from *Pglyrp2*$^{+/-}$ ceca infected with *Salmonella* at 48 h by flow cytometry. The analysis of GFP expression in CD8$^+$ TCRβ$^+$ cells from the IEL compartment showed significantly increased expression of PGLYRP2 ($P = 0.04$) following infection (Fig. 2B). A similar increase in expression ($P = 0.05$) was noted in CD8$^+$ TCRγδ$^+$ cells although this corresponded to a minor IEL population (Fig. 2B). On the other hand, no significant difference in GFP-PGLYRP2 expression was observed in cells from the LPL compartment (Fig. 2C). It appears that IEL CD8$^+$ TCRβ$^+$ lymphocytes, the most abundant subset found among cecal leukocyte populations, also displayed the most prominent increase in the expression of PGLYRP2 following *Salmonella* infection. Together, these results establish that PGLYRP2 is readily induced in specific immune cell subsets of the intestinal mucosa in response to enteric infection with *Salmonella*, thus suggesting a role for this peptidoglycan-interacting molecule in host defense *in vivo*.

PGLYRP2 does not play a role in an early Nod1/2-dependent Th17 response to *Salmonella* infection. As shown above, PGLYRP2 is expressed in the immune cell population of the intestinal mucosa, and *Pglyrp2* mRNA levels are significantly elevated in this tissue in response to *Salmonella* infection (Fig. 1 and 2). We then speculated that PGLYRP2, through its capacity to bind or to hydrolyze peptidoglycan, may serve as a modulator of Nod1/2-dependent host defense in response to *Salmonella* infection. Therefore, we investigated the putative role of PGLYRP2 in Th17-dependent inflammation in *Salmonella* colitis because this arm of the host response to *Salmonella* was shown to depend on Nod1 and Nod2 (8, 9). To this end, WT and *Pglyrp2*$^{-/-}$ (KO) mice were treated with streptomycin and infected with 5×10^7 CFU of SL1344. Mice were sacrificed at 24 h, 48 h, or 72 h following infection, and then their ceca were homogenized for analysis. qRT-PCR analysis of *Il17a* and *Il22* from WT and *Pglyrp2*$^{-/-}$ cecum revealed no significant changes in their expression over the period of infection (Fig. 3A). Moreover, the expression of *Lcn2* (encoding lipocalin 2) and *RegIIIγ* (encoding regenerating islet-derived IIIγ), the antimicrobial proteins important for interleukin-22 (IL-22)-dependent mucosal defense against enteric bacteria (26), did not change significantly in the cecum of *Pglyrp2*$^{-/-}$ mice compared to that of WT mice (Fig. 3B).

Nod1 and Nod2 regulate the levels of key inflammatory cytokines such as the keratinocyte-derived chemokine (KC) and IL-1β during *Salmonella* colitis (8). Therefore, we assessed the impact of PGLYRP2 on the expression of the cytokines *KC* and *Il1β* during

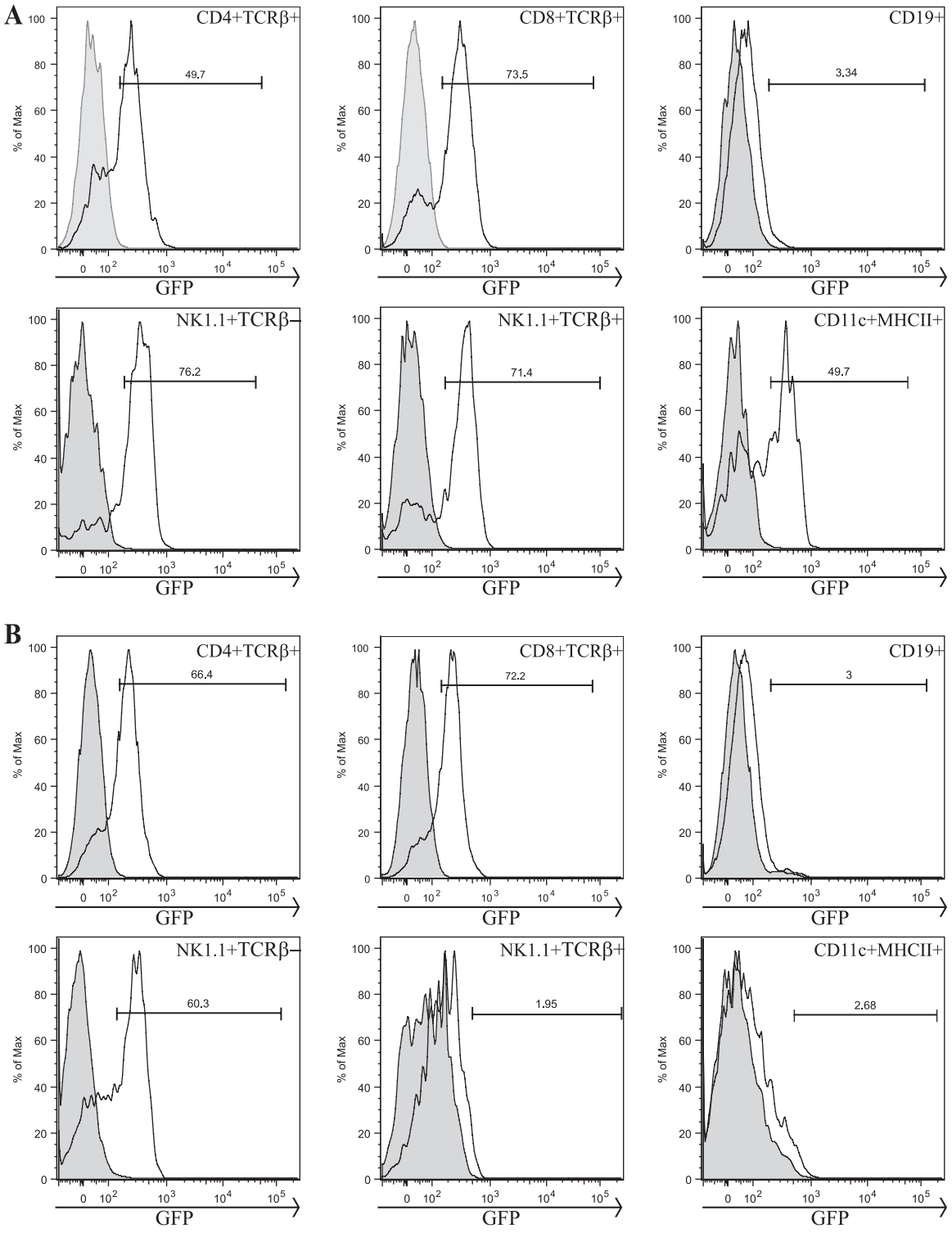

FIG 1 Analysis of PGLYRP2 expression in intestinal cellular subsets. IELs and LPLs were prepared from cecal samples of wild-type and *Pglyrp2*$^{+/-}$ mice, stained with various surface markers (CD4$^+$, TCRβ$^+$, CD8$^+$, CD19$^+$, NK1.1$^+$, and CD11c$^+$), and analyzed by flow cytometry for GFP expression. Histograms show expression of GFP$^+$ cells on gated subsets (CD4$^+$ TCRβ$^+$, CD8$^+$ TCRβ$^+$, CD19$^+$, NK1.1$^+$ TCRβ$^+$, NK1.1$^+$ TCRβ$^-$, and CD11c$^+$ MHC-II$^+$) from IELs (A) and LPLs (B). The percentage of GFP-expressing cells in *Pglyrp2*$^{+/-}$ mice was determined using wild-type cells as a baseline (shaded area). One representative of three experiments is shown; three mice were pooled for each group.

TABLE 1 Detailed characterization of the cecal leukocyte population expressing the reporter gene carrying GFP under the control of the *Pglyrp2* promoter at steady state

Cecal cell type in *Pglyrp2*$^{+/-}$ mice	% of GFP-expressing cells[a]	
	IELs	LPLs
CD4$^+$ TCRβ$^+$	47.6 ± 2.0	56.7 ± 9.7
CD8$^+$ TCRβ$^+$	70.1 ± 2.0	74.5 ± 2.5
CD8$^+$ TCRγδ$^+$	33.0 ± 10	13.3 ± 3.3
NK1.1$^+$ TCRβ$^-$	78.5 ± 2.3	64 ± 4.0
NK1.1$^+$ TCRβ$^+$	70.3 ± 4.1	3.4 ± 1.1
CD19$^+$	3.9 ± 2.0	3.3 ± 0.7
CD11b$^+$ CD11c$^-$ Gr1$^+$	1.7 ± 1.7	<1.0
CD11b$^+$ CD11c$^-$ Gr1$^-$	<1.0	<1.0
CD11c$^+$ MHC-II$^+$	35.2 ± 10.0	<1.0
CD11b$^+$ CD11c$^+$	23.5 ± 13.9	<1.0

[a] Data shown are the mean ± standard error of the mean of three independent experiments.

infection. qRT-PCR analysis from WT and *Pglyrp2*$^{-/-}$ cecal samples showed no significant differences in the mRNA levels of these inflammatory cytokines (Fig. 3C), suggesting that, unlike Nod1 and Nod2, PGLYRP2 expression does not have an impact on the level of these inflammatory cytokines during *Salmonella* infection. Overall, these findings indicate that PGLYRP2 does not modulate Nod1- and Nod2-dependent early Th17 inflammatory responses during *Salmonella* colitis.

***Pglyrp2*-deficient mice have increased inflammation in the cecum following *Salmonella* infection.** Although PGLYRP2 does not appear to affect the Nod1/2-dependent Th17 inflammatory responses, this does not exclude a possibility that PGLYRP2 may still play a role independent of Nod1 and Nod2 in *Salmonella* colitis. To test this hypothesis, we stained cecum samples from uninfected and infected WT and *Pglyrp2*$^{-/-}$ mice and performed histological analysis. The analyzed features included polymorphonuclear leukocyte (PMN) accumulation, goblet cell depletion, edema, and epithelial erosion, which were blindly scored using a previously established scoring system (see Materials and Methods) (Fig. 4A). Although infected *Pglyrp2*$^{-/-}$ mice displayed no change in cecal inflammation compared to infected wild-type mice at early stages of infection (24 to 48 h) (Fig. 4A and B), we noticed that the level of infiltrating PMNs was significantly higher in *Pglyrp2*$^{-/-}$ mice than in WT mice at 48 h postinfection ($P = 0.04$) (Fig. 4C). Moreover, goblet cell depletion was also significantly elevated at 48 h postinfection in *Pglyrp2*$^{-/-}$ mice relative to WT mice ($P = 0.01$) (Fig. 4D). Despite the absence of significant differences at early time points of infection, we observed at 72 h postinfection a marked increase in cecal inflammation in *Pglyrp2*$^{-/-}$ mice ($P = 0.02$) (Fig. 4A and B). This was reflected by significantly enhanced PMN recruitment and goblet cell depletion in infected *Pglyrp2*$^{-/-}$ mice compared to WT mice ($P = 0.03$, and 0.003, respectively) (Fig. 4C and D). It must be noted that this increase in pathology did not follow the pathology seen in

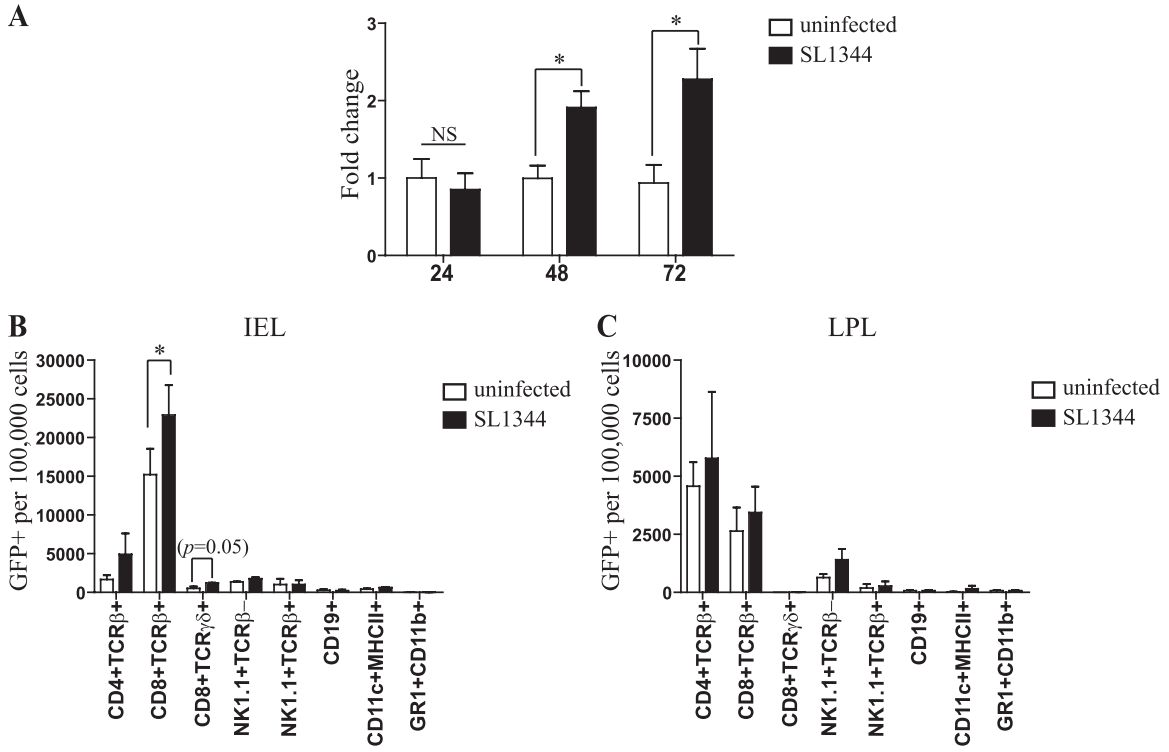

FIG 2 *Pglyrp2* expression is increased in the cecum following *Salmonella* infection. qRT-PCR was used to measure the expression of *Pglyrp2* in the ceca from uninfected and infected WT mice at 24 h, 48 h, and 72 h (A). The expression is normalized to the housekeeping gene *Rpl19* (6 to 8 mice per group per experiment) ($n = 3$; *, $P < 0.05$). The bar graph shows average fold change over uninfected controls ($n = 3$). The average relative frequency of GFP$^+$ cells in different populations (CD4$^+$ TCRβ$^+$, CD8$^+$ TCRβ$^+$, CD8$^+$ TCRγδ$^+$, NK1.1$^+$ TCRβ$^-$, NK1.1$^+$ TCRβ$^+$, CD19$^+$, CD11c$^+$ MHC-II$^+$, and Gr1$^+$ CD11b$^+$) in cecal IELs (B) and LPLs (C) from *Pglyrp2*$^{+/-}$ mice uninfected or 48 h after infection with SL1344 was quantified by flow cytometry analysis ($n = 3$; *, $P < 0.05$).

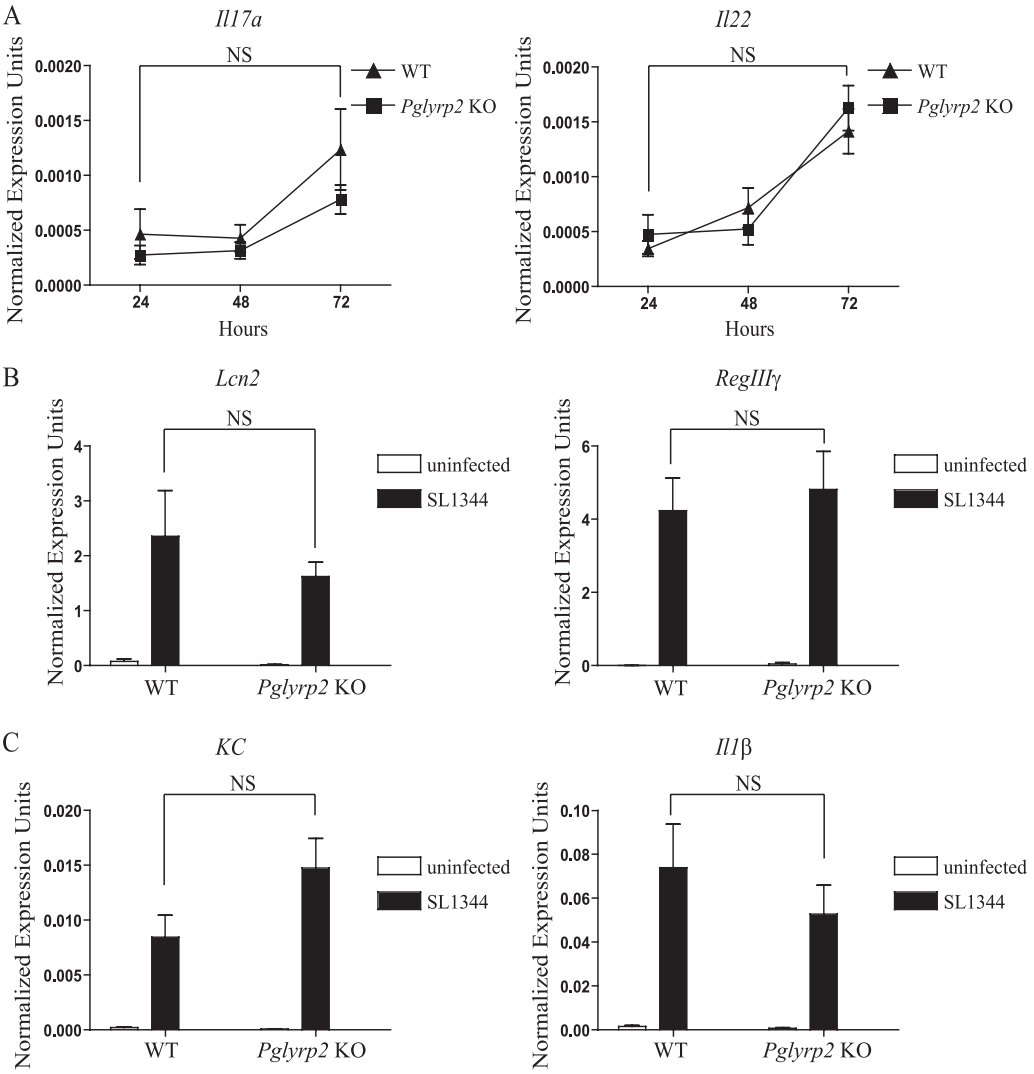

FIG 3 PGLYRP2 does not modulate Nod-dependent early Th17 responses or inflammatory cytokine responses to *Salmonella* infection. qRT-PCR was used to measure the mRNA level of *Il17a* and *Il22* (A), *Lcn2* and *RegIII*γ (B), and *KC* and *Il1*β (C) in cecal samples from streptomycin-treated WT and *Pglyrp2*$^{-/-}$ (KO) mice infected with 5×10^7 CFU of SL1344 for 24 to 72 h. Line graphs in panel A show the average expression levels of *Il17a* and *Il22* in infected samples over time. Bar graphs depict the average expression levels of antimicrobial peptides (B) and inflammatory cytokines (C) in both uninfected and infected samples at 72 h. The expression is normalized to the housekeeping gene *Rpl19* (6 to 8 mice per group per experiment). One representative of three experiments is shown. Error bars represent 1 standard error of the mean. NS, not significant.

Nod1$^{-/-}$ *Nod2*$^{-/-}$ double knockout (DKO) mice, where inflammation is significantly reduced following infection (8). Finally, spleens and cecal tissue samples were examined from the same infected mice as those used for histological analysis to determine bacterial colonization and spread. Although *Pglyrp2*$^{-/-}$ mice had levels of colonization similar to those of WT mice in both spleen and cecum samples, a trend toward increased bacterial load ($P = 0.07$) was observed in *Pglyrp2*$^{-/-}$ cecal tissues at 72 h postinfection compared to WT cecal tissues (Fig. 4E and F). Thus, our findings indicate that PGLYRP2 plays a protective role during the late stage of *Salmonella* colitis and that this role is independent of Nod1- and Nod2-induced control of inflammation.

Cecal inflammation is greatly exacerbated in *Nod2*$^{-/-}$ *Pglyrp2*$^{-/-}$ DKO mice following 24 h postinfection with *Salmonella* SL1344. Next, we sought to investigate whether PGLYRP2 differentially influence Nod1 or Nod2 response to bacterial peptidoglycan *in vivo*. In order to carry out the investigation, we first crossed our *Pglyrp2*$^{-/-}$ mice with either *Nod1*$^{-/-}$ or *Nod2*$^{-/-}$ mice to generate the double knockout (DKOs) *Nod1*$^{-/-}$ *Pglyrp2*$^{-/-}$ and *Nod2*$^{-/-}$ *Pglyrp2*$^{-/-}$ mice. We then performed histological analysis on the cecum samples from uninfected and infected WT, *Pglyrp2*$^{-/-}$, *Nod1*$^{-/-}$ *Pglyrp2*$^{-/-}$ DKO, and *Nod2*$^{-/-}$ *Pglyrp2*$^{-/-}$ DKO mice at 24 h. The individual pathological features were scored (Fig. 5A) and were subsequently combined to calculate the average pathological scores (Fig. 5B). Infected *Nod1*$^{-/-}$ *Pglyrp2*$^{-/-}$ DKO mice displayed no significant change ($P = 0.12$) in cecal inflammation compared to that of infected WT or *Pglyrp2*$^{-/-}$ mice at 24 h (Fig. 5B). Interestingly, however, we observed that the level of cecal inflammation was greatly elevated ($P = 0.005$) in *Nod2*$^{-/-}$ *Pglyrp2*$^{-/-}$ DKO mice at 24 h p.i. with *Salmonella* (Fig. 5B). This increase was attributed to a significantly higher level of infiltrating PMNs ($P = 0.003$), as well

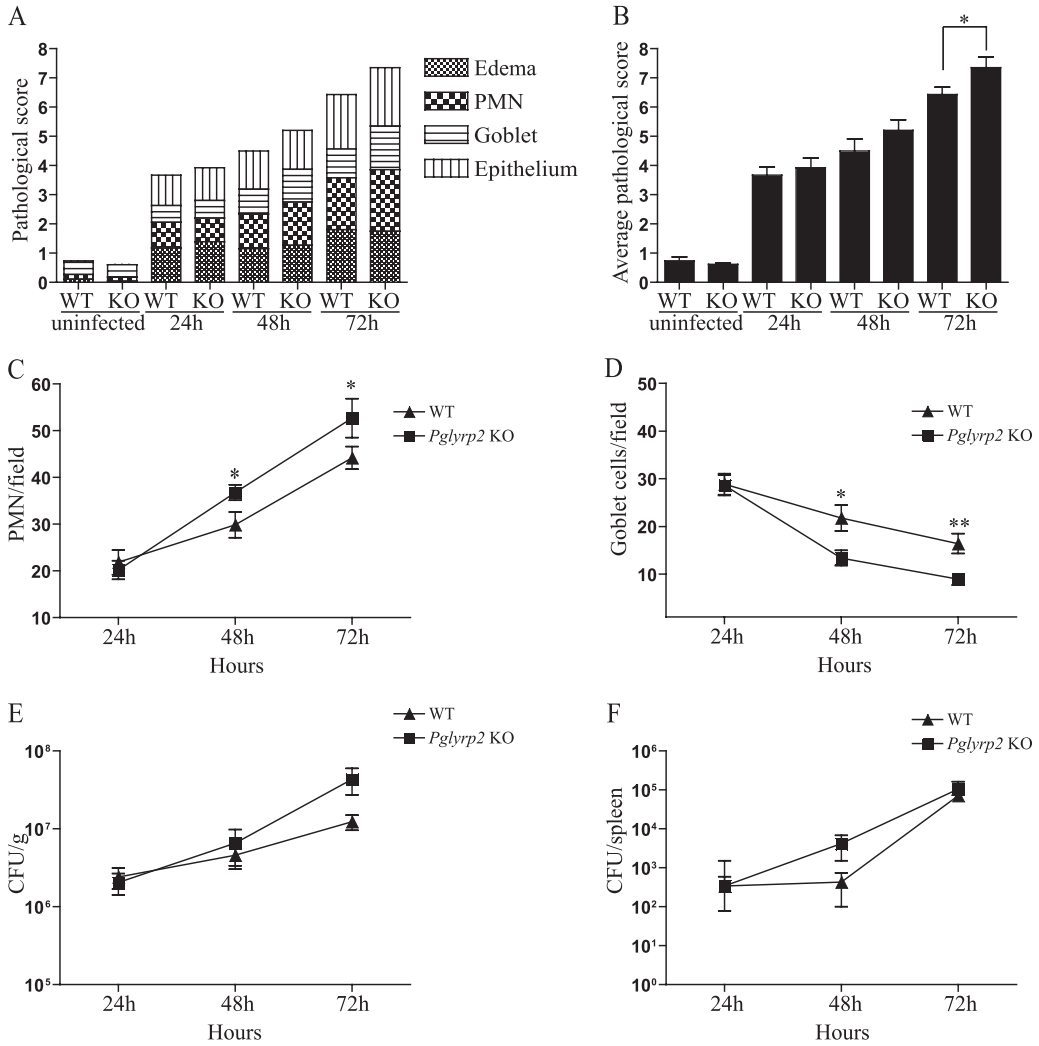

FIG 4 *Pglyrp2*$^{-/-}$ mice have increased inflammation following SL1344 infection. Streptomycin-treated WT or *Pglyrp2*$^{-/-}$ (KO) mice were either PBS treated (uninfected) or infected with 5×10^7 CFU of SL1344 for 24 to 72 h; then, their ceca were examined for histological changes and bacterial loads. For histological changes, the average pathological scores for each analyzed feature (edema, neutrophil recruitment, goblet cell depletion, and epithelial erosion) for all mice from each group were calculated (A) as well as the average total sum of the pathological scores (B). The line graphs depict the average numbers of PMNs (C) and goblet cells (D) observed per microscopic field from infected samples over the period of infection. For bacterial loads, CFU counts were determined on cecal tissue (E) and spleen (F) samples from infected mice ($n = 3$; 6 to 8 mice per group per experiment). Error bars represent 1 standard error of the mean. *, $P < 0.05$; **, $P < 0.01$.

as an increased percentage of submucosal edema ($P = 0.005$) in the cecal tissue of *Nod2*$^{-/-}$ *Pglyrp2*$^{-/-}$ DKO mice compared to that of the WT mice (Fig. 5C and D). In contrast, goblet cell depletion did not seem to contribute to this enhanced phenotype as no difference was observed in the levels from the ceca of either WT or *Nod2*$^{-/-}$ *Pglyrp2*$^{-/-}$ DKO mice (data not shown). Finally, both *Nod1*$^{-/-}$ *Pglyrp2*$^{-/-}$ DKO and *Nod2*$^{-/-}$ *Pglyrp2*$^{-/-}$ DKO mice had levels of colonization similar to those of WT mice in both spleen and cecum samples at 24 h postinfection (Fig. 5E and F). In conclusion, *Nod2*$^{-/-}$ *Pglyrp2*$^{-/-}$ DKO mice seem to have an exacerbated inflammatory response to *Salmonella* infection relative to that of *Nod1*$^{-/-}$ *Pglyrp2*$^{-/-}$ DKO mice, suggesting that PGLYRP2 may differentially regulate the response by Nod1 and Nod2 to bacterial peptidoglycan and that Nod2 signaling is likely intact and confers early protection against *Salmonella* infection in *Pglyrp2*$^{-/-}$ mice.

DISCUSSION

In the present study, we investigated the role of PGLYRP2 in *Salmonella enterica* serovar Typhimurium-induced colitis. We found that *Pglyrp2* expression was increased in the cecum of *Salmonella*-infected mice, and, by flow cytometry, we observed that expression of GFP under control of the *Pglyrp2* promoter was increased in discrete populations of cecal lymphocytes, in response to infection. Our results also demonstrated that PGLYRP2 did not contribute to the expression of Th17-associated cytokines, IL-22-dependent antimicrobial proteins, or inflammatory cytokines. However, *Pglyrp2*-deficient mice displayed significantly enhanced inflammation in the cecum at 72 h postinfection, reflected by increased PMN infiltration and goblet cell depletion, thus showing for the first time a role for PGLYRP2 in the host defense against an enteric bacterial pathogen *in vivo*. Moreover, *Nod2*$^{-/-}$ *Pglyrp2*$^{-/-}$

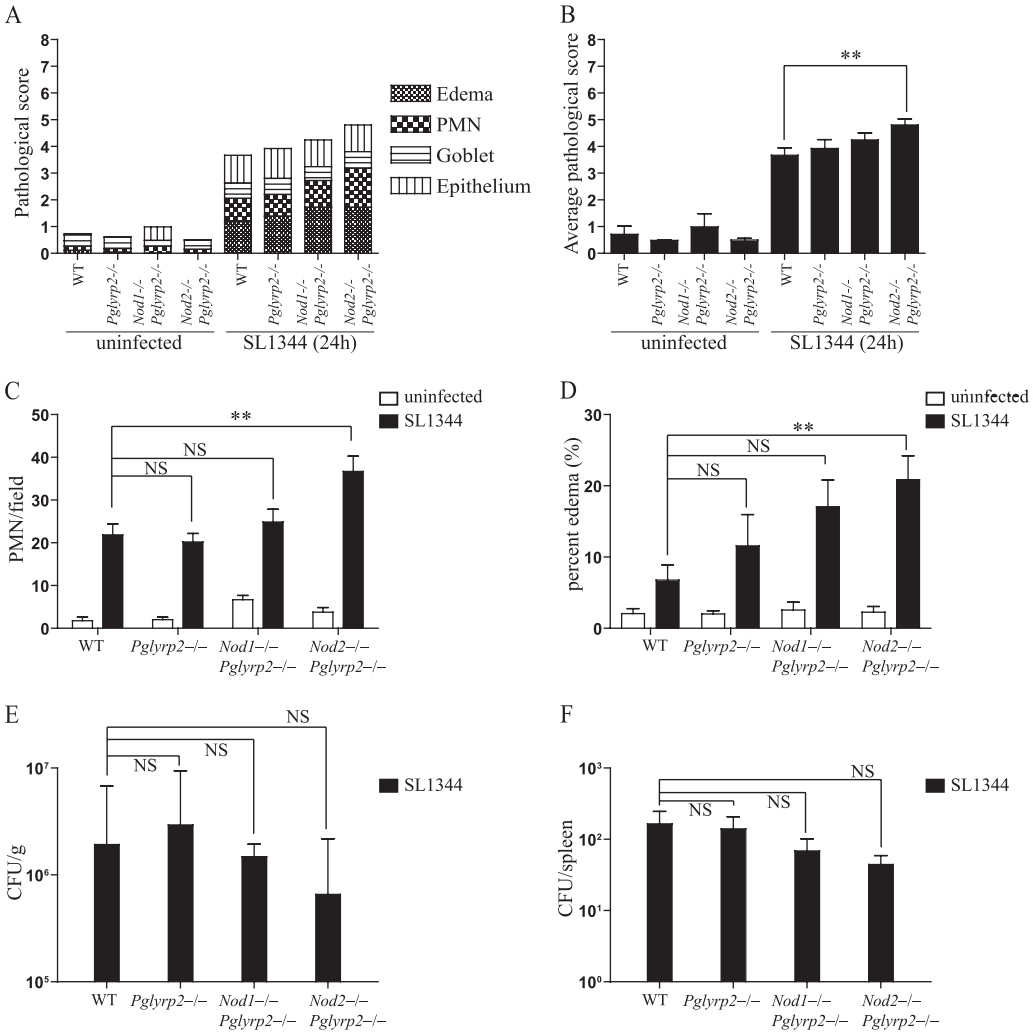

FIG 5 *Nod2*$^{-/-}$ *Pglyrp2*$^{-/-}$ mice have significantly increased inflammation at 24 h following SL1344 infection. Streptomycin-treated WT, *Pglyrp2*$^{-/-}$, *Nod1*$^{-/-}$ *Pglyrp2*$^{-/-}$, and *Nod2*$^{-/-}$ *Pglyrp2*$^{-/-}$ mice were either PBS treated (uninfected) or infected with 5×10^7 CFU of SL1344 for 24 h; then, their ceca were examined for histological changes and bacterial loads. For histological changes, the average pathological scores for each analyzed feature (edema, PMN recruitment, goblet cell depletion, and epithelial erosion) for all mice from each group were calculated (A) as well as the average total sum of the pathological scores (B). The line graphs depict the average numbers of PMNs (C) and the percentage of submucosal edema (D) observed per microscopic field from infected samples over the period of infection. For bacterial loads, CFU counts were determined on cecal tissue (E) and spleen (F) samples from infected mice ($n = 3$; 6 to 8 mice per group per experiment). Error bars represent 1 standard error of the mean. *, $P < 0.05$; **, $P < 0.01$; NS, nonsignificant.

DKO mice displayed highly elevated levels of inflammation at an earlier time point (24 h p.i.) than WT, *Pglyrp2*$^{-/-}$, and *Nod1*$^{-/-}$ *Pglyrp2*$^{-/-}$ DKO mice, suggesting intricate and complex relationships among these PRMs.

The processing and degradation of peptidoglycan by host enzymes such as PGLYRP2 and lysozyme can indirectly influence bacterial sensing by pattern recognition receptors, such as Nod1 and Nod2. While lysozyme cleaves the sugar chain between GlcNAc (*N*-acetylglucosamine) and *N*-acetylmuramic acid (MurNAc), PGLYRP2 specifically hydrolyzes the lactyl bond between MurNAc and L-Ala, generating free peptide fragments, which are nonetheless still recognized by Nod1 (such as the tripeptide L-Ala-D-Glu-*meso*-DAP or the tetrapeptide L-Ala-D-Glu-*meso*-DAP-D-Ala) (14, 22). Similarly, PGLYRP2 was shown to hydrolyze the lysine-containing muramyl tripeptide MurNAc-L-Ala-D-Glu-Lys into L-Ala-D-Glu-Lys (39), which can no longer be recognized by Nod2 (14). Interestingly, the minimum peptidoglycan fragments hydrolyzed by PGLYRP2 are muramyl tripeptides (containing either *meso*-DAP or Lys), and therefore the typical Nod2 ligand MDP is not cleaved by PGLYRP2 (39), suggesting that MDP could remain biologically active to stimulate Nod2 regardless of the presence or absence of PGLYRP2. For this reason, it is likely that the hydrolytic activity of PGLYRP2 is not sufficient to functionally degrade Nod1/2-specific peptidoglycan fragments *in vivo* although this has not been directly tested. In particular, it remains possible that, although MurNAc-L-Ala-D-Glu-*meso*-DAP and L-Ala-D-Glu-*meso*-DAP can activate Nod1 with similar capacities, the presence of the sugar moiety could modify cellular uptake, as we recently suggested (19). It is also possible that PGLYRP2 could differentially affect Nod2-dependent responses to bacteria, depending on the relative proportions of dipeptide versus Lys-containing tripeptides in their peptidoglycan, a ratio

that varies from one bacterial species to another. Nevertheless, these considerations strongly suggest that the amidase activity of mammalian PGLYRP2 may not be responsible for promoting a global scavenger function aiming to dampen immune responses dependent on peptidoglycan. This contrasts with the role assigned to *Drosophila* amidase PGRPs, such as PGRP-LB. Indeed, in *Drosophila* detection of peptidoglycan and induction of innate immune responses to bacteria by effector PGRPs (such as PGRP-LC or PGRP-SA) require that peptidoglycan fragments contain both sugar and peptide moieties (17, 31).

In our *Salmonella* infection model, it appears that PGLYRP2 may trigger host defense and innate immune responses independently of its amidase activity, especially given that our histology data on infected mice did not follow the pathology observed in *Nod1*$^{-/-}$ *Nod2*$^{-/-}$ double knockout mice where inflammation is significantly reduced during infection (8). Supporting this argument, an immune-modulatory role for PGLYRP2 irrespective of its amidase function has been recently shown in the arthritis inflammation model (30). In this study, the authors showed that both Nod2 and PGLYRP2 were required for the induction of peptidoglycan-induced arthritis and that Nod2 was acting upstream of PGLYRP2 to induce its expression. Indeed, our data support the notion that Nod proteins and PGLYRP2 may be working together to promote protection in our colitis model. In our study, we observed at an early stage (24 h) of *Salmonella* infection a significant increase in cecal inflammation in *Nod2*$^{-/-}$ *Pglyrp2*$^{-/-}$ DKO mice, but not *Nod1*$^{-/-}$ *Pglyrp2*$^{-/-}$ DKO mice, compared to inflammation in WT or *Pglyrp2*$^{-/-}$ mice. Our data thus suggest that both Nod2 and PGLYRP2 may be working in concert as part of a regulatory pathway, where contribution of Nod1 is minimal, to confer protection during *Salmonella* infection. These results are also in agreement with the previous biochemical data mentioned above, which demonstrated that PGLYRP2 was unable to degrade MDP, the muramyl peptide agonist of Nod2 (39).

In summary, we have demonstrated a protective role for PGLYRP2 during *Salmonella* infection *in vivo*, and this represents the first indication that this molecule contributes to the host defense against bacterial pathogens at mucosal surfaces. Although it is clear that PGLYRP2 plays a protective role in downregulating inflammation in *Salmonella*-induced colitis, whether this effect is mediated by amidase-dependent processing of peptidoglycan fragments and affects Nod1/2-driven host responses is questionable, given that PGLYRP2 did not seem to modulate Nod1/2-dependent, early Th17 responses to *Salmonella* infection. Further research is required to delineate the mechanisms by which PGLYRP2 confers protection in the intestine during bacterial infection.

ACKNOWLEDGMENTS

This work was supported by Canadian Institutes of Health Research (CIHR) and the Howard Hughes Medical Institute (to D.J.P.) and by CIHR and the Crohn's and Colitis Foundation of Canada (to S.E.G.).

REFERENCES

1. **Barreau F, et al.** 2007. CARD15/NOD2 is required for Peyer's patches homeostasis in mice. PLoS One **2**:e523. doi:10.1371/journal.pone.0000523.
2. **Barthel M, et al.** 2003. Pretreatment of mice with streptomycin provides a *Salmonella enterica* serovar Typhimurium colitis model that allows analysis of both pathogen and host. Infect. Immun. **71**:2839–2858.
3. **Chamaillard M, et al.** 2003. An essential role for NOD1 in host recognition of bacterial peptidoglycan containing diaminopimelic acid. Nat. Immunol. **4**:702–707.
4. **Duerr CU, et al.** 2011. Control of intestinal Nod2-mediated peptidoglycan recognition by epithelium-associated lymphocytes. Mucosal Immunol. **4**:325–334.
5. **Dziarski R, Platt KA, Gelius E, Steiner H, Gupta D.** 2003. Defect in neutrophil killing and increased susceptibility to infection with nonpathogenic gram-positive bacteria in peptidoglycan recognition protein-S (PGRP-S)-deficient mice. Blood **102**:689–697.
6. **Fritz JH, Ferrero RL, Philpott DJ, Girardin SE.** 2006. Nod-like proteins in immunity, inflammation and disease. Nat. Immunol. **7**:1250–1257.
7. **Geddes K, Magalhaes JG, Girardin SE.** 2009. Unleashing the therapeutic potential of NOD-like receptors. Nat. Rev. **8**:465–479.
8. **Geddes K, et al.** 2010. Nod1 and Nod2 regulation of inflammation in the *Salmonella* colitis model. Infect. Immun. **78**:5107–5115.
9. **Geddes K, et al.** 2011. Identification of an innate T helper type 17 response to intestinal bacterial pathogens. Nat. Med. **17**:837–844.
10. **Gelius E, Persson C, Karlsson J, Steiner H.** 2003. A mammalian peptidoglycan recognition protein with *N*-acetylmuramoyl-L-alanine amidase activity. Biochem. Biophys. Res. Commun. **306**:988–994.
11. **Girardin SE, et al.** 2003. Nod1 detects a unique muropeptide from gram-negative bacterial peptidoglycan. Science **300**:1584–1587.
12. **Girardin SE, et al.** 2003. Nod2 is a general sensor of peptidoglycan through muramyl dipeptide (MDP) detection. J. Biol. Chem. **278**:8869–8872.
13. **Girardin SE, Philpott DJ.** 2004. Mini-review: the role of peptidoglycan recognition in innate immunity. Eur. J. Immunol. **34**:1777–1782.
14. **Girardin SE, et al.** 2003. Peptidoglycan molecular requirements allowing detection by Nod1 and Nod2. J. Biol. Chem. **278**:41702–41708.
15. **Hapfelmeier S, Hardt WD.** 2005. A mouse model for *S. typhimurium*-induced enterocolitis. Trends Microbiol. **13**:497–503.
16. **Inohara N, et al.** 2003. Host recognition of bacterial muramyl dipeptide mediated through NOD2. Implications for Crohn's disease. J. Biol. Chem. **278**:5509–5512.
17. **Kaneko T, et al.** 2004. Monomeric and polymeric gram-negative peptidoglycan but not purified LPS stimulate the *Drosophila* IMD pathway. Immunity **20**:637–649.
18. **Kashyap DR, et al.** 2011. Peptidoglycan recognition proteins kill bacteria by activating protein-sensing two-component systems. Nat. Med. **17**:676–683.
19. **Lee J, et al.** 2009. pH-dependent internalization of muramyl peptides from early endosomes enables Nod1 and Nod2 signaling. J. Biol. Chem. **284**:23818–23829.
20. **Lu X, et al.** 2006. Peptidoglycan recognition proteins are a new class of human bactericidal proteins. J. Biol. Chem. **281**:5895–5907.
21. **Ma P, Wang Z, Pflugfelder SC, Li DQ.** 2010. Toll-like receptors mediate induction of peptidoglycan recognition proteins in human corneal epithelial cells. Exp. Eye Res. **90**:130–136.
22. **Magalhaes JG, et al.** 2005. Murine Nod1 but not its human orthologue mediates innate immune detection of tracheal cytotoxin. EMBO Rep. **6**:1201–1207.
23. **Magalhaes JG, Tattoli I, Girardin SE.** 2007. The intestinal epithelial barrier: how to distinguish between the microbial flora and pathogens. Semin. Immunol. **19**:106–115.
24. **Osanai A, et al.** 2011. Mouse peptidoglycan recognition protein PGLYRP-1 plays a role in the host innate immune response against *Listeria monocytogenes* infection. Infect. Immun. **79**:858–866.
25. **Paredes JC, Welchman DP, Poidevin M, Lemaitre B.** 2011. Negative regulation by amidase PGRPs shapes the *Drosophila* antibacterial response and protects the fly from innocuous infection. Immunity **35**:770–779.
26. **Raffatellu M, et al.** 2009. Lipocalin-2 resistance confers an advantage to *Salmonella enterica* serotype Typhimurium for growth and survival in the inflamed intestine. Cell Host Microbe **5**:476–486.
27. **Rakoff-Nahoum S, Paglino J, Eslami-Varzaneh F, Edberg S, Medzhitov R.** 2004. Recognition of commensal microflora by toll-like receptors is required for intestinal homeostasis. Cell **118**:229–241.
28. **Royet J, Dziarski R.** 2007. Peptidoglycan recognition proteins: pleiotropic sensors and effectors of antimicrobial defences. Nat. Rev. Microbiol. **5**:264–277.
29. **Saha S, et al.** 2010. Peptidoglycan recognition proteins protect mice from experimental colitis by promoting normal gut flora and preventing induction of interferon-gamma. Cell Host Microbe **8**:147–162.
30. **Saha S, et al.** 2009. PGLYRP-2 and Nod2 are both required for peptidoglycan-induced arthritis and local inflammation. Cell Host Microbe **5**:137–150.

31. **Stenbak CR, et al.** 2004. Peptidoglycan molecular requirements allowing detection by the *Drosophila* immune deficiency pathway. J. Immunol. **173**: 7339–7348.
32. **Tydell CC, Yount N, Tran D, Yuan J, Selsted ME.** 2002. Isolation, characterization, and antimicrobial properties of bovine oligosaccharide-binding protein. A microbicidal granule protein of eosinophils and neutrophils. J. Biol. Chem. **277**:19658–19664.
33. **Tydell CC, Yuan J, Tran P, Selsted ME.** 2006. Bovine peptidoglycan recognition protein-S: antimicrobial activity, localization, secretion, and binding properties. J. Immunol. **176**:1154–1162.
34. **Uehara A, et al.** 2005. Chemically synthesized pathogen-associated molecular patterns increase the expression of peptidoglycan recognition proteins via toll-like receptors, NOD1 and NOD2 in human oral epithelial cells. Cell Microbiol. **7**:675–686.
35. **Uematsu S, Fujimoto K.** 2010. The innate immune system in the intestine. Microbiol. Immunol. **54**:645–657.
36. **Vanderwinkel E, de Pauw P, Philipp D, Ten Have JP, Bainter K.** 1995. The human and mammalian *N*-acetylmuramyl-L-alanine amidase: distribution, action on different bacterial peptidoglycans, and comparison with the human lysozyme activities. Biochem. Mol. Med. **54**:26–32.
37. **Wang H, Gupta D, Li X, Dziarski R.** 2005. Peptidoglycan recognition protein 2 (*N*-acetylmuramoyl-L-Ala amidase) is induced in keratinocytes by bacteria through the p38 kinase pathway. Infect. Immun. **73**:7216–7225.
38. **Wang M, et al.** 2007. Human peptidoglycan recognition proteins require zinc to kill both gram-positive and gram-negative bacteria and are synergistic with antibacterial peptides. J. Immunol. **178**:3116–3125.
39. **Wang ZM, et al.** 2003. Human peptidoglycan recognition protein-L is an *N*-acetylmuramoyl-L-alanine amidase. J. Biol. Chem. **278**:49044–49052.
40. **Xu M, Wang Z, Locksley RM.** 2004. Innate immune responses in peptidoglycan recognition protein L-deficient mice. Mol. Cell. Biol. **24**:7949–7957.
41. **Yoshida H, Kinoshita K, Ashida M.** 1996. Purification of a peptidoglycan recognition protein from hemolymph of the silkworm, *Bombyx mori*. J. Biol. Chem. **271**:13854–13860.
42. **Zaidman-Remy A, et al.** 2006. The *Drosophila* amidase PGRP-LB modulates the immune response to bacterial infection. Immunity **24**:463–473.
43. **Zhang Y, et al.** 2005. Identification of serum *N*-acetylmuramoyl-L-alanine amidase as liver peptidoglycan recognition protein 2. Biochim. Biophys. Acta **1752**:34–46.